Quantifying defects in ceramic tight ultra- and nanofiltration membranes and investigating their robustness

Kramer, F. C.; Shang, R.; Scherrenberg, S. M.; Rietveld, L. C.; Heijman, S. J.G.

DOI
10.1016/j.seppur.2019.03.019

Publication date
2019

Document Version
Final published version

Published in
Separation and Purification Technology

Separation and Purification Technology 219 (2019) 159–168

Contents lists available at ScienceDirect

Separation and Purification Technology

journal homepage: www.elsevier.com/locate/seppur

Quantifying defects in ceramic tight ultra- and nanofiltration membranes and investigating their robustness

F.C. Kramer[a,*], R. Shang[a,*], S.M. Scherrenberg[b], L.C. Rietveld[a], S.J.G. Heijman[a]

[a] Department of Sanitary Engineering, Faculty of Civil Engineering and Geosciences, Delft University of Technology, P.O. Box 5048, 2600 GA Delft, the Netherlands
[b] Evides N.V., P.O. Box 4472, 3006 AL Rotterdam, the Netherlands

ARTICLE INFO

Keywords:
Ceramic membranes
Water treatment
Molecular weight cut-off
Defects
Sodium hypochlorite

ABSTRACT

One of the perceived benefits of ceramic membranes is their robustness, which makes them suitable for treating high organic load waste streams. In particular, ceramic tight ultrafiltration (tUF) and nanofiltration (NF) form an important barrier against small colloids and organic molecules. In order to achieve this barrier, the quality of the membranes should be uncompromised.

An extension on a commonly used size exclusion method was developed in order to quantify defects in membranes and calculate the MWCO accurately excluding the defects. This approach gives a better representation of the membrane quality than the original method. The quality of a broad range of commercial ceramic membranes was investigated by determining the (i) hydraulic permeability, (ii) molecular weight cut-off, and (iii) quantitative defects. Several membranes – both tubular and disc membranes, selected from various suppliers – were tested to investigate their variability. Furthermore, the robustness of tubular NF membranes was studied by monitoring the effect of long-term exposure to sodium hypochlorite, which is commonly used to mitigate organic fouling.

The results showed that batches of both tubular and disc membranes of different pore size and suppliers included membranes with defects. Furthermore, the long-term treatment of tubular ceramic membranes with sodium hypochlorite negatively affected, beyond expectation, the quality of the membranes. The separation layer in these membranes was not notably compromised by sodium hypochlorite exposure, but the end seal layer was damaged.

1. Introduction

Due to their robustness, ceramic membranes have become more popular in water treatment applications over the last decade. These membranes are not only perceived to be resistant to high pressure, temperature, and concentrations of chemicals but also to have a homogeneous distribution of narrow pores and a long lifetime [1–4].

Ceramic membranes have proven to be effective for drinking water treatment [2]. In literature, studies can also be found on the treatment of water streams with a high organic load originating from various industries, such as the treatment of textile industry waste streams, both on the laboratory [1,5,6] and pilot scale [7]. In addition, the pulp and paper industry has interest in the use of ceramic membranes since its wastewater is one of the major sources of industrial water pollution. The main goal is to recover residual lignin, organic matter and water [8–11]. Furthermore, much research is conducted in the oil and gas industry [11–16] as well as in the vegetable oil industry [11,15]. Lastly, ceramic membranes are forthcoming for sewage treatment [17,18] or its effluent [19] and for seawater desalination, specifically as pre-treatment for reverse osmosis [20–23].

A major advantage of using ultrafiltration (UF) or nanofiltration (NF) for the treatment of high organic load waste streams is that UF/NF forms a barrier against small colloids and organic molecules, which are abundantly present in those waste streams. Therefore, the quality of ceramic membranes is of utmost importance and should be monitored accurately and regularly.

Several quality tests were reported, which can be divided into direct and indirect quality methods; methods that will analyse the membrane itself and methods that will monitor the water quality of the permeate water, respectively [24]. The most commonly used direct methods for microfiltration membranes are a pressure decay test (PDT) and a diffusive airflow (DAF) test, which are simple and reliable but must be monitored off-line. Indirect methods include particle counting, turbidity monitoring, and size exclusion methods can be performed online

* Corresponding authors.
E-mail addresses: francakramer@gmail.com (F.C. Kramer), r.shang@tudelft.nl (R. Shang).

https://doi.org/10.1016/j.seppur.2019.03.019
Received 25 July 2018; Received in revised form 12 January 2019; Accepted 5 March 2019
Available online 06 March 2019
1383-5866/

Table 1
Overview of tested ceramic tUF and NF membranes.

Purchased cut-off	Geometry	Length or diameter	Filtration area	Pore size	Porosity	Glass seal layer	Filtration layer	Total membranes tested
450 Da	Tubular	100 mm	0.163 dm^2	0.9 nm	30–40%	Yes	TiO_2	29 (3 batches)
450 Da	Disc	85 mm	0.563 dm^2	0.9 nm	30–40%	No	TiO_2	14 (1 batch)
1000 Da	Disc	85 mm	0.563 dm^2	1 nm	30–40%	No	TiO_2	10 (1 batch)
2000 Da	Disc	85 mm	0.563 dm^2	3 nm	30–55%	No	ZrO_2	3 (1 batch)
3000 Da	Disc	85 mm	0.563 dm^2	5 nm	30–55%	No	TiO_2	4 (1 batch)

[25].

For analysing the quality of ceramic UF or NF membranes, size exclusion and permporometry methods are most commonly used [26–28]. The disadvantage to permporometry is the requirement of specific equipment [28–30]. When using size exclusion methods, the molecular weight cut-off (MWCO) is determined using a multiple monodisperse molecules of different sizes, e.g. polyethylene glycol (PEG) molecules [31]. By using a mixture of PEG molecules only a single filtration experiment is needed to calculate the MWCO which can only be successfully achieved when using high accuracy in detection, e.g. with High Performance Liquid Chromatography (HPLC). However, the size exclusion method has its limits. When a MWCO higher than the MWCO according to the specifications of the supplier (from now on referred to as the *purchased cut-off*) is measured, the distinction between enlarged pore sizes (larger than the purchase cut-off) and potential cracks or gaps in the membrane cannot be made. The cracks and gaps, defined as defects on the membrane surface, cause short circuiting of the feed water to the permeate; when these defects occur, the quality of the membranes is compromised. This existing method will average the overall pore size with the defects in the membranes, which will not give a good representation of the overall pore size of the membrane. Therefore, a new method is required to quantify the defects in the membrane to be able to determine whether the membrane is compromised which will be presented in this paper.

Other encounter of the exclusion method is the effect of pore-plugging by large PEG molecules. When pore-plugging occurs, large sized PEG molecules block the (enlarged) pores or the gaps and cracks, resulting in a lower calculated MWCO than the actual MWCO. This can be prevented by keeping the range of the PEG molecules as small as possible. Therefore, we set guidelines in this paper to prevent pore-plugging to occur.

Thibault et al. found that when using ceramic membranes during the recovery and recycling of oil sands produced water, linear defects on the filtration layer occurred [12]. The study noted these linear defects were likely induced by solvent evaporation during the fabrication of the selective layer using the sol–gel method [12,32]. Furthermore, Buekenhoudt reviewed stability of porous ceramic membranes especially the corrosion and thermal instabilities [33]. They found that microporous TiO_2 membranes sintered at 450 °C showed no significant membrane degradation during dynamic corrosion tests using cross-flow filtration [4,33]. However, only the chemicals used for the dynamic corrosion tests were limited to HNO_3 (pH 2–3) and NaOH (pH 11–13). Other studies on the quality and robustness of ceramic tight ultrafiltration (tUF) and NF membranes are limited, according to the authors' knowledge.

Sodium hypochlorite is widely used for chemical cleaning in order to remove organic and inorganic fouling from membranes [2,6,17,21,23]. However, there are few long-term studies on the effect of this chemical treatment in literature. Almecija et al. showed that long-term treatment with a caustic surfactant solution at a temperature of 60 °C damaged ceramic MF membranes made of ZrO_2-TiO_2 [34]. Conversely, van Gestel et al. reported a long-term chemical resistance of ceramic NF membranes between pH 1.5 and 13 using HNO_3 for acidification and NaOH for alkalisation with an exposure time of six weeks [4]. Studies on the long-term effect of hypochlorite have not yet been reported in literature.

Thus, the main purpose of this research was (i) to develop a suitable method to quantitatively analyse the defects in ceramic membranes in order to investigate the quality and (ii) to investigate the long-term robustness of commercially manufactured ceramic tUF and NF membranes. This information is essential to outline the potential of these membranes for the treatment of high organic load waste streams.

Firstly, the quality of the membranes was determined by investigating the (i) hydraulic permeability, (ii) MWCO of the membranes, and (iii) quantitative defects. Sixty membranes, both tubular and disc membranes, with different MWCOs from various suppliers were investigated.

Secondly, the robustness of the membranes over long-term testing was studied by exposing tubular NF membranes to 100 h of sodium hypochlorite cleanings, which is the equivalent of one year of operation with regular chemical cleaning. Furthermore, the pore size distribution and defects were measured by determining the MWCO of the membranes before and after each experiment.

2. Materials and methods

2.1. Membranes

A total of sixty ceramic tUF and NF membranes, both tubular and disc membranes from various suppliers, with a purchased cut-off ranging from 450 Da to 3000 Da were tested (Table 1). The following definitions were used based on the MWCO of the membranes: ceramic membranes with a MWCO between 500 Da and 3000 Da were defined as tUF membranes, and those with a MWCO smaller than 500 Da as NF membranes [17,18,35]. The tubular membranes had a silica glass seal of 13 mm on the edges of the membranes to prevent feed water from entering the permeate side (Fig. 1). The glass seal was not present for disc membranes because the feed and permeate were separated by an O-ring. The disc membranes were housed in the Spirlab INSIDE DISRAM™ (TAMI) disc holder with a diameter of 90 mm.

2.2. Hydraulic permeability

The hydraulic permeability of the ceramic tUF and NF membranes was determined by filtration in cross-flow mode using demineralised water at room temperature with a duration of 1 h. During these tests, the flow was measured continuously and the trans-membrane pressure (TMP) was kept constant at 4 bar. As recommended by the suppliers, the cross-flow velocity was between 1.0 and 1.2 m/s for tubular and 6.0–7.0 m/s for disc membranes. Both cross-flow velocities correspond to turbulent flow conditions which minimises the effect of concentration polarisation. Within 10 min, the hydraulic permeability became constant, and the reported values are the average of these constant values. In order to correct for the temperature, the following equation was used to calculate the permeability:

$$L_{20Â°C} = \frac{J \cdot e^{-0.0239 \cdot (T-20)}}{\Delta P} \quad (1)$$

where, $L_{20\ °C}$ is the temperature-corrected permeability at 20 °C ($L \cdot (m^2 \cdot h \cdot bar)^{-1}$), T is temperature of water (°C), J is membrane flux ($L \cdot (m^2 \cdot h \cdot bar)^{-1}$), and ΔP is transmembrane pressure (bar). All permeability values were temperature-corrected to 20 °C [36].

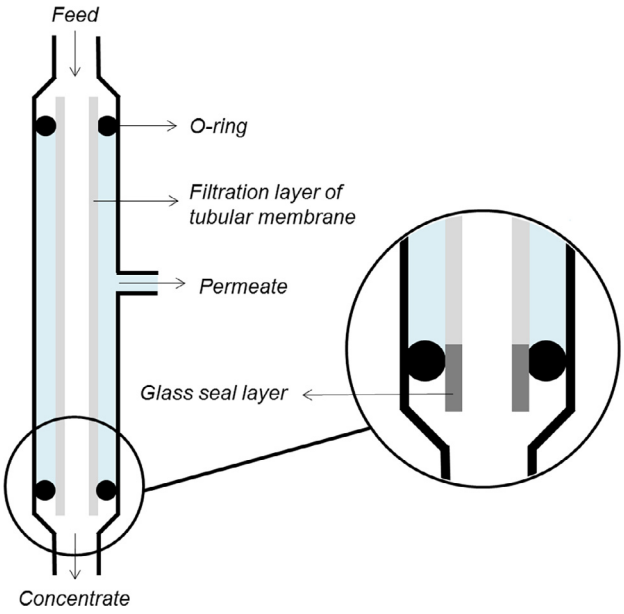

Fig. 1. Illustration of the tubular membranes in the membrane module during filtration. The detailed illustration shows the glass seal layer at the edges of the tubular membrane. These glass seal layers prevent the feed from short-circuiting to the permeate side via the support layer of the membrane.

2.3. MWCO analysis

2.3.1. MWCO calculation

The MWCO and hydraulic permeability of pristine ceramic tUF and NF membranes were measured to determine the quality of the membranes. Tam & Tremblay (1991) described that with a five component mixture of PEGs, the MWCO of membranes can accurately be determined [37]. This method is widely used for the determination of the pore size distribution of membranes [26–28].

The MWCO was investigated by filtering a mixture of five different PEGs (0.2–6 kDa) (Sigma-Aldrich) each in a concentration of 6 mg·L^{-1}. Similar settings were used as described for the hydraulic permeability. The range of the PEGs, $PEG_{n=1}$ to $PEG_{n=5}$, was selected based on the purchased cut-off of the membranes (Eqs. (2) and (3), Table 2). It's imperative to keep the PEG range as small as possible to prevent pore plugging by large PEG molecules.

$$PEG_{n=1} \leq \frac{1}{2} \cdot MWCO_{membrane} \tag{2}$$

$$PEG_{n=5} \geq 2 \cdot MWCO_{membrane} \tag{3}$$

The feed and permeate samples were analysed using HPLC (Shimadzu) equipped with size exclusion chromatography columns (SEC, 5 µm 30 Å PSS SUPREMA) and a RID-20A refractive index detector. Ultrapure water was used as carrier liquid in the HPLC at a flow rate of 1 mL·min^{-1}. The molecular weight distribution curves of the dissolved PEG molecules in the feed and permeate, derived from the HPLC analyses, were transformed into retention curves by calculating the rejection percentage of a PEG with a certain molecular weight (R_i) using Eq. (4):

$$R_i(\%) = \left(\frac{c_{i,feed} - c_{i,permeate}}{c_{i,feed}} \right) \cdot 100\% \tag{4}$$

where, $c_{i,\ feed}$ and $c_{i,\ permeate}$ are the PEG concentration in the feed and the permeate samples. Afterwards, the experimental retention curves were described by a log-normal model as function of MW and MWCO using Eq. (5) [26,27,38]. Eq. (5) was used to model retention curve (see Fig. 2) to be able to calculate the MWCO.

$$\sigma(MW_s) = \int_0^{MW_s} \frac{1}{s_{MW}\sqrt{2\pi}} \cdot \frac{1}{MW} \cdot exp\left[-\frac{(\ln(MW) - \ln(MWCO) + 0.56 \cdot s_{MW})^2}{2 \cdot s_{MW}^2} \right] \cdot dMW \tag{5}$$

where, $\sigma(MW_s)$ is the reflection coefficient for a PEG with a molecular weight MW_s, s_{MW} is the standard deviation of the molecular weight distribution.

It is assumed that the separation of the PEG molecules is only based on size exclusion with negligible solute diffusion. Therefore, the molecular size of the PEG solutes (d_s in nm) is correlated to their molecular weight (MW in Da) as shown in Eq. (6) [26,38].

$$d_s = 0.065 \cdot MW^{0.438} \tag{6}$$

The MWCO was estimated at 90% of the retention curve [27,36]. Fig. 2 shows an example of a retention curve derived from the HPLC data.

Table 2
Content of the PEG mixture used during MWCO analysis for each purchased cut-off.

Purchased cut-off	PEG mixture
450 Da	200, 300, 400, 600, 1000 Da
1000 Da	600, 1000, 1500, 2000, 3000 Da
2000 Da	1000, 1500, 3000, 4000, 6000 Da
3000 Da	1000, 1500, 3000, 4000, 6000 Da

2.3.2. Corrected MWCO calculation

The MWCO calculation described in the previous section is commonly used for membrane research. However, it is not applicable for membranes with defects. Defects are (small) gaps or cracks in the membrane with a size larger than the largest PEG molecule used in the test, as illustrated in Fig. 3. Defects can occur in the filtration layer and/or the glass seal layer on the edge of the membrane (Fig. 1). Fig. 2 shows the PEG-retention curve of a membrane with defects. The retention curve does not reach 100%, meaning that not all of the largest PEG-molecules are rejected by the membrane. Due to defects, PEG molecules with a MW larger than the pore size of the membrane will be able to pass the membrane (Figs. 2 and 3). Therefore, we developed an extension to the MWCO calculation in order to correct for the defects. In this calculation, it is defined that the defects are the percentage of the largest PEG molecule passing through the membrane, which is also the percentage of feed water leaked to the permeate via the defects. Thus, the percentage of defects can be calculated with Eq. (7):

$$defects(\%) = (1 - R_{PEG,n=5}) \cdot 100\% \tag{7}$$

where $R_{PEG,\ n=5}$ is the rejection rate of the largest PEG molecule by the membrane. For example, it can be concluded from Fig. 2 that 30% of the PEGs passed the defect(s) in the membrane. By correcting the rejection curve to 100%, an estimation of the rejection of the filtration layer is given (Fig. 2). Thus, the defects are excluded to be able to calculate the overall MWCO of the filtration layer without the defects, while also quantifying defects. Fig. 3 illustrates the derivation of the rejection percentage from Eq. (4) to Eq. (8) for the mass balance, where the rejection rate is corrected for defects ($R_{i,\ d}$). Eq. (8) is found below:

$$R_{i,d}(\%) = \left(\frac{c_{i,feed} - (c_{i,permeate} + c_{i,feed} \cdot (1 - R_{PEG,n=5}))}{c_{i,feed}} \right) \cdot 100\% \tag{8}$$

where, $c_{i,\ feed}$ and $c_{i,\ permeate}$ are the PEG concentrations in the feed and the permeate samples, respectively, and $R_{PEG,\ n=5}$ is the removal rate of the largest PEG molecules, permeating through the defects. $1 - R_{PEG,\ n=5}$ represents the ratio of the largest PEG molecules flowing through the defects (Fig. 3). This equation can be simplified to Eq. (9).

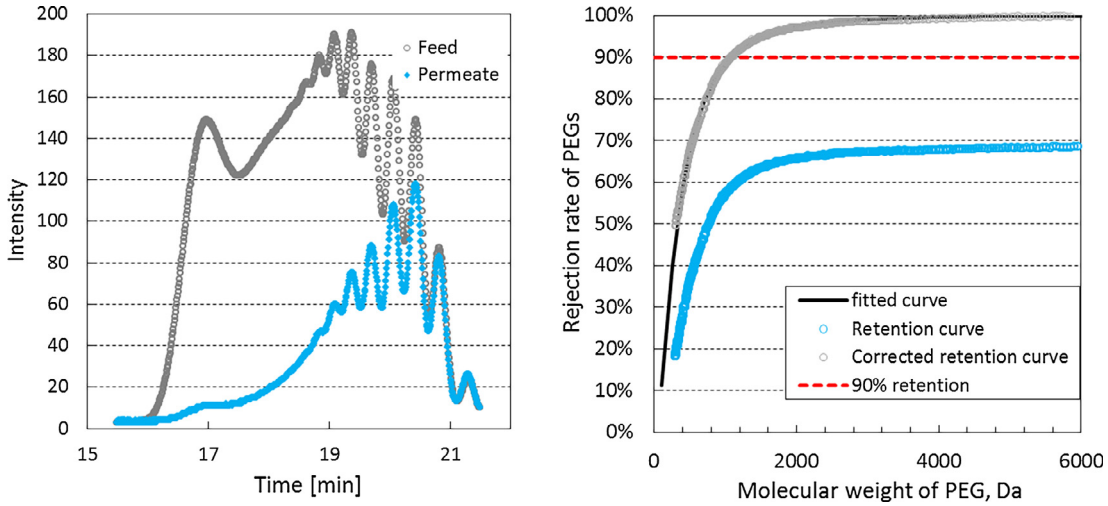

Fig. 2. (a–b): (a) Output of the HPLC: the intensity versus time for a feed and permeate sample of a membrane with a purchase cut-off of 450 Da. The difference between feed and permeate was large indicating a high retention of PEG's; no defects were measured in this membrane. The retention was calculated using Eqs. (4) or (9). (b) The original and corrected retention curve of a pristine disc membrane with a purchased cut-off of 1 kDa, calculated with HPLC data and Eqs. (4) or (9). The fitted curve was derived from Eqs. (5) and (6). It was not possible to determine the MWCO from the original graph because the retention curve never reaches 90% retention due to the defects in this membrane. Using the MWCO calculation with correction for defects (corrected graph) makes it possible to calculate the MWCO of this membrane with defects.

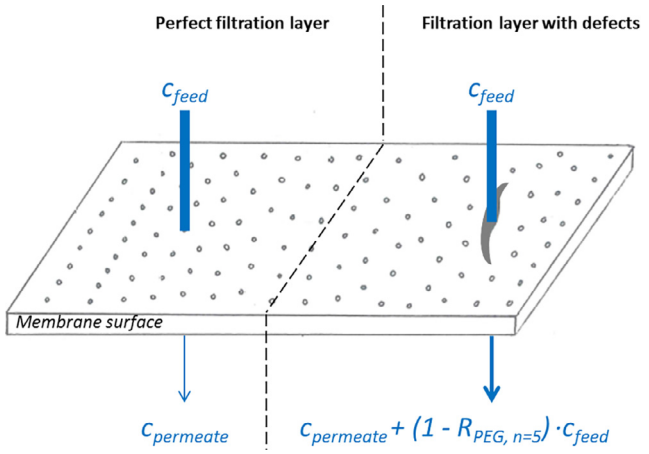

Fig. 3. Illustration of the concentration of PEGs passing the membrane surface based on the mass balance for membranes without (left side) and with (right side) defects. When defects occur in the membrane, a greater amount of PEG compounds can pass the membrane to the permeate side. This should be taken into account when calculating the MWCO of the membrane filtration layer.

$$R_{i,d}\,(\%) = \left(\frac{c_{i,feed} \cdot R_{PEG,n=5} - c_{i,permeate}}{c_{i,feed}}\right) \cdot 100\% \tag{9}$$

The corrected rejection percentage of a PEG with a certain molecular weight ($R_{i,\ corrected}$) used for membranes with defects was calculated using Eq. (10).

$$R_{i,corrected}\,(\%) = \left(\frac{R_{i,d}}{R_{PEG,n=5}}\right) \cdot 100\% \tag{10}$$

It must be noted that the corrected MWCO only corrects for defects larger than the largest PEG used for the analysis, $PEG_{n=5}$ (Eqs. (7), (8) and (10)). Due to this assumption, smaller sized defects were not accounted for in this calculation. These smaller sized defects would range between the pore size and the largest PEG used for the analysis.

2.4. Chemical cleaning

The effect of long-term chemical cleaning with sodium hypochlorite on the tubular ceramic NF membranes was investigated because it is known as the most effective cleaning agent for (organically) fouled ceramic membranes [2,6,17,21]. The permeability and MWCO were tested after 100 h of chemical cleaning with 1% sodium hypochlorite to simulate the cleaning intensity of one year of operation, assuming five days of continuous filtration followed by 1.33 h of chemical cleaning with 1% sodium hypochlorite for 365 days [17]. These concentrations were within the specifications of the supplier. In addition, a more intense chemical cleaning was tested, using 2% sodium hydroxide at 97 °C for 30 min.

2.5. Applying epoxy glue on the edges of the tubular membranes

After chemical cleaning, the edges of the tubular membranes were sealed again with a two-component epoxy glue, Araldite 2020. Fig. 1 illustrates the glass seal layer at the edges of the tubular membranes. The resulting glued layer was microscopically examined to ensure that the edges were properly sealed.

3. Results and discussion

3.1. Quality of pristine ceramic tUF and NF membranes

An extension on the commonly used size exclusion method described by Tam and Tremblay (1991) was developed to be able to quantify defects in membranes and accurately calculate the MWCO excluding the defects. In this section, the MWCO values of the extended method (*corrected MWCO*) and the original MWCO method (*uncorrected MWCO*) were compared. The uncorrected MWCO calculation gives an average of the overall pore size of the membrane, including the potential defects. Whereas, the corrected MWCO calculation gives a represents the overall pore size by excluding the defects in the calculation for the MWCO while also quantifying the defects present in the membrane. Thus, the corrected MWCO together with the defects gives a better representation of the quality of the membrane. This method is described in the Materials & Methods.

In this section, the quality of sixty pristine ceramic tUF and NF membranes was analysed by measuring the MWCO, hydraulic permeability, and defects. The results of three batches of pristine ceramic NF membranes with a purchased cut-off of 450 Da were compared (Fig. 4).

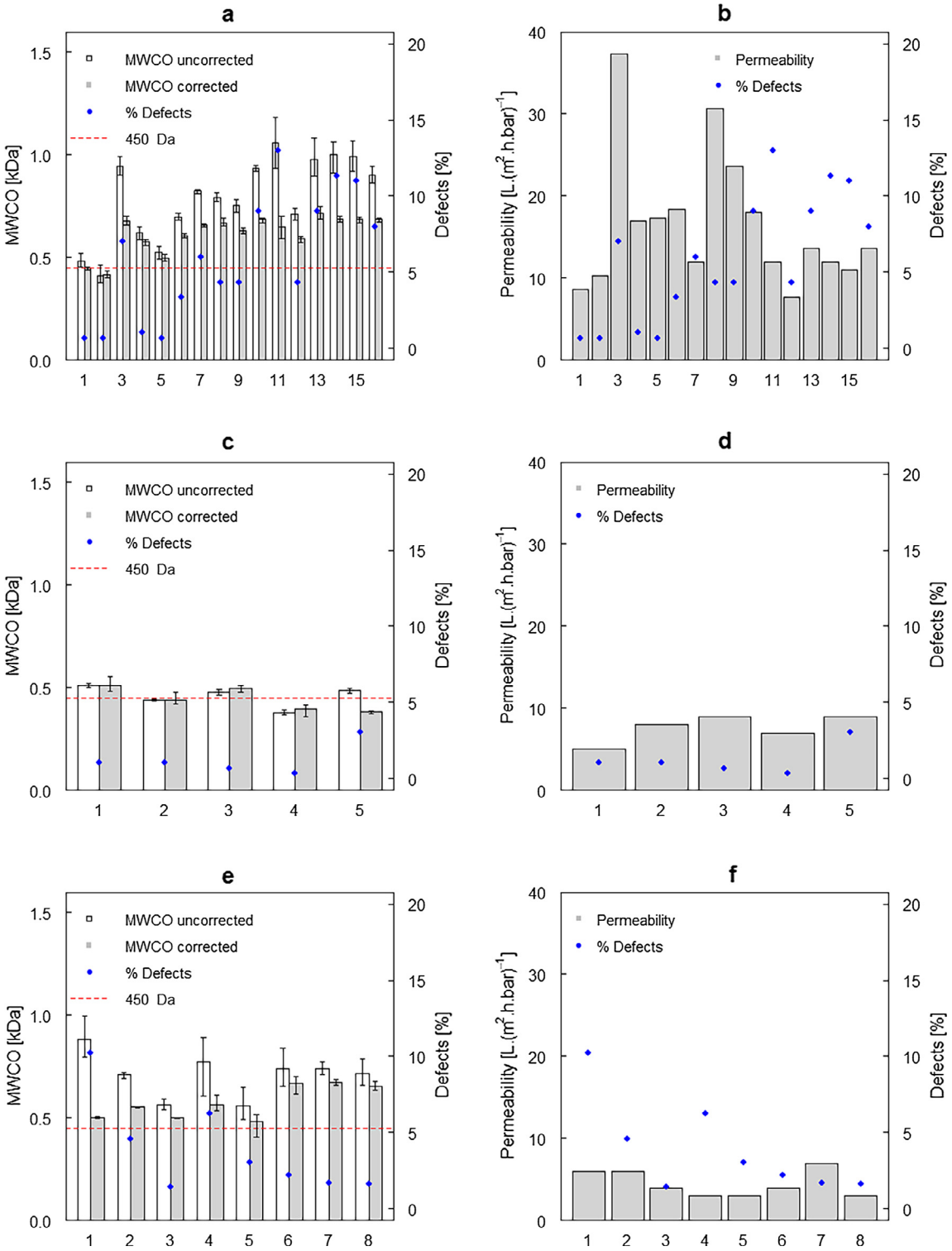

Fig. 4. (a–f): MWCO in kDa (left) and hydraulic permeability in $L{\cdot}(m^2{\cdot}h{\cdot}bar)^{-1}$ (right) of pristine ceramic NF membranes. MWCO of tubular membranes with a purchased cut-off of 450 Da (red dashed line) was calculated without (white bars) and with correction for defects (grey bars). The percentages of defects in the membrane are shown (blue dots). The error bars represent the standard deviation of triplicate measurements. Three different batches are shown consisting of 16, 5, and 8 membranes, respectively. (For interpretation of the references to colour in this figure legend, the reader is referred to the web version of this article.)

The defects were shown in the graph with the both the MWCO and the permeability data, to be able to compare. First, there is a notable variation in the (i) uncorrected and corrected MWCO, (ii) hydraulic permeability, and (iii) percentage of defects measured in the pristine membranes, even within one batch. This indicates that the production process is not consistent for these tested batches.

Second, the graphs in Fig. 4 show that a higher percentage of defects in the membranes led, as expected, to a higher uncorrected MWCO. There was a clear relation between the uncorrected MWCO and defects: this is visible in Fig. 5a. A higher percentage of defects also led to a higher corrected MWCO, even though the defects are excluded in this calculation. This means that defects occurred in the range between 450

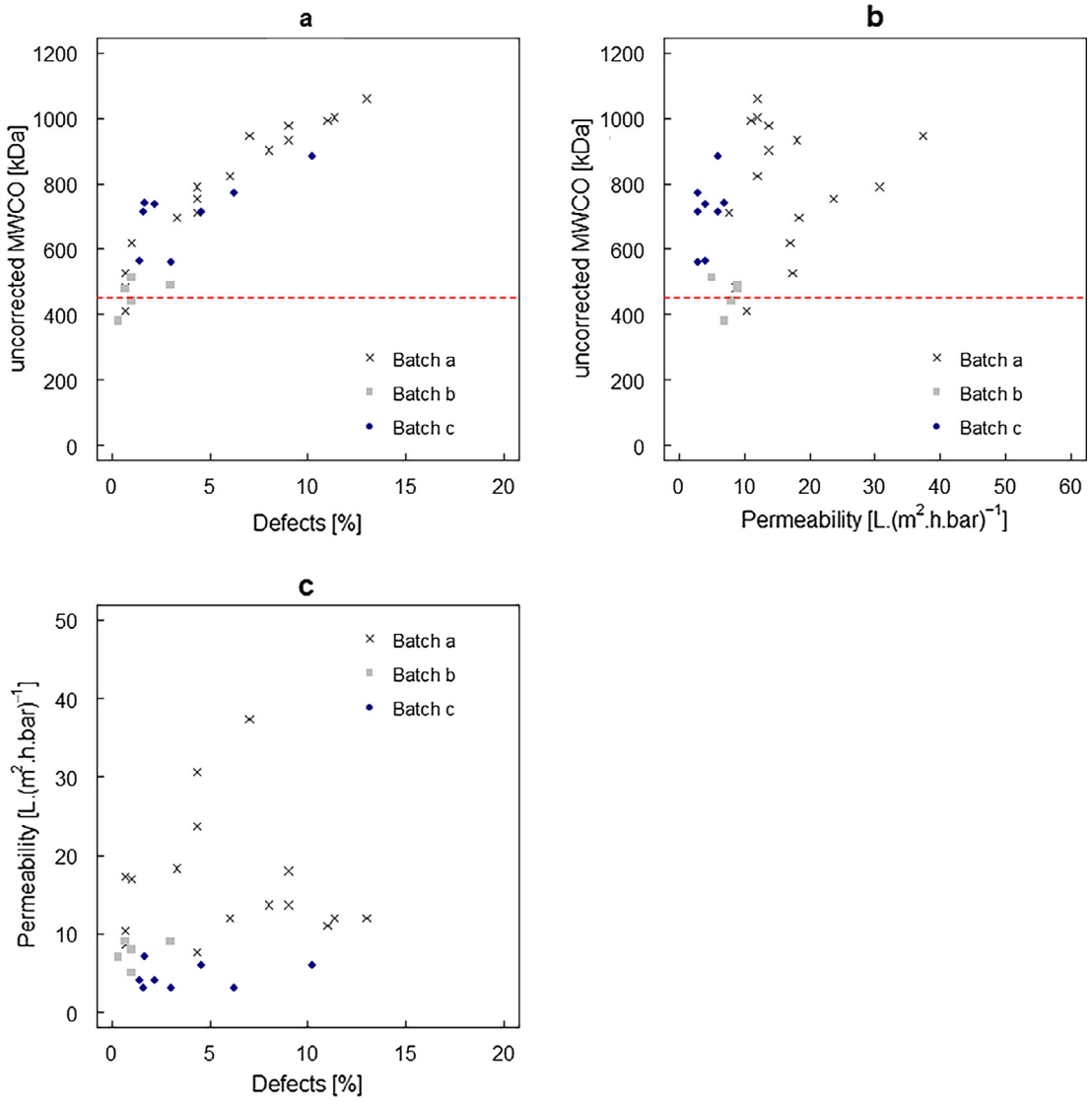

Fig. 5. (a–c): Uncorrected MWCO in kDa versus (a) the permeability in $L{\cdot}(m^2{\cdot}h{\cdot}bar)^{-1}$ and (b) percentage of defects. (c) Permeability versus the percentage of defects. The graphs show data of tubular membranes with a purchased cut-off of 450 Da (red dashed line). Three batches are shown consisting of 16, 5, and 8 membranes. (For interpretation of the references to colour in this figure legend, the reader is referred to the web version of this article.)

and 1000 Da, and defects in this range were not excluded from the MWCO calculation as explained in the Materials & Methods.

Third, the hydraulic permeability varied between 5 and 37 $L{\cdot}(m^2{\cdot}h{\cdot}bar)^{-1}$ (Fig. 4b, d, f). This could also be explained by the occurrence of defects on the membrane surface; the feed solution can pass the membrane surface more easily through the defects, leading to a higher permeability. However, the results in Fig. 5c show no clear relation between the permeability and the percentage of defects for the twenty-nine tubular 450 Da membranes tested. Moreover, there was also no direct link between the uncorrected MWCO and the permeability (Fig. 5b). Another explanation for the increase in permeability is the variation in thickness of the filtration layer. Fig. 10 shows an electron microscopy photo with variations of 1.4–2.4 µm of filtration layer thickness on the ceramic membranes with a purchased cut-off of 3 kDa. According to the Carman-Kozeny relation, the thickness of the filtration layer exhibits an inverse linear relationship with the permeability [36]. So, a thinner filtration layer thickness leads to a higher permeability. This indicates variation in the filtration layer thickness of the analysed pristine membranes.

Next, membranes with a different geometry, disc membranes, were compared to the tubular ceramic NF membranes. First, disc membranes with a purchased cut-off of 450 Da were tested (Fig. 6). The results were better than the tubular ceramic NF membranes; 13 out of 14 disc membranes contained less than 2% defects, whereas one membrane had 6% defects (Fig. 6).

In addition, disc membranes with a purchased cut-off of 1 kDa were tested, with defects ranging from 4 to 18%. The corrected MWCO ranged from 1.1 to 1.4 kDa, with permeabilities between 77 and 210 $L{\cdot}(m^2{\cdot}h{\cdot}bar)^{-1}$ (Fig. 7). The three disc membranes with a purchased cut-off of 2 kDa showed no defects. However, the corrected MWCO ranged between 3 and 4 kDa, which indicates that the pores of these membranes were considerably larger than the purchased cut-off. The hydraulic permeability was about 150 $L{\cdot}(m^2{\cdot}h{\cdot}bar)^{-1}$ for all tested membranes (Fig. 8). The highest percentage of defects were measured in disc membranes with a purchased cut-off of 3 kDa, where defects ranged between 10 and 61% and permeability ranged from 23 to 82 $L{\cdot}(m^2{\cdot}h{\cdot}bar)^{-1}$ (Fig. 9).

3.2. Robustness of ceramic NF membranes

The robustness of the ceramic membranes was investigated by exposing the membranes to sodium hypochlorite for the equivalent of one

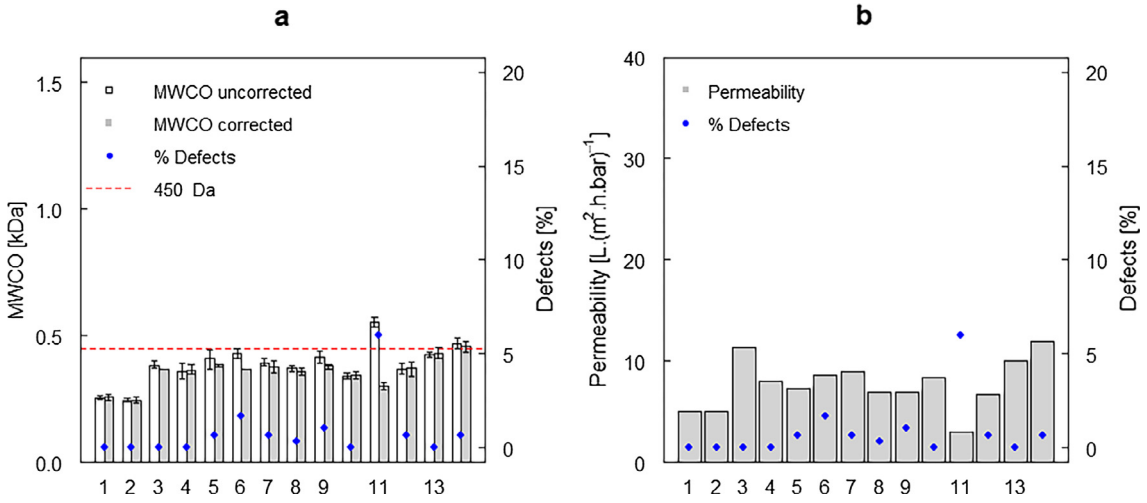

Fig. 6. (a–b): MWCO in kDa (a) and hydraulic permeability in $L\cdot(m^2\cdot h\cdot bar)^{-1}$ (b) of pristine ceramic NF membranes. MWCO of disc membranes with a purchased cut-off of 450 Da (red dashed line) was calculated without (white bars) and with correction for defects (grey bars). The percentages of defects in the membrane are shown (blue dots). The error bars represent the standard deviation of triplicate measurements. One batch is shown. (For interpretation of the references to colour in this figure legend, the reader is referred to the web version of this article.)

year of chemical cleaning. Results showed that long-term treatment with sodium hypochlorite caused a considerable increase of the MWCO and hydraulic permeability (Fig. 11). In this section the corrected MWCO method was used to calculate the corrected MWCO and the defects, since these represent the membrane condition the best. The four pristine ceramic NF membranes used for this experiment had a corrected MWCO between 482 and 566 Da, defects lower than 7%, and a hydraulic permeability ranging between 3.2 and 5.7 $L\cdot(m^2\cdot h\cdot bar)^{-1}$. After 100 h of sodium hypochlorite treatment, the percentages of defects in all of the membranes increased up to 16%. Moreover, the corrected MWCO increased to 769–799 Da. Thus, this increase in MWCO was caused by the occurrence of additional defects, in the range of the pore size of the membrane (Fig. 11a). Furthermore, the increase in hydraulic permeability to 32–41 $L\cdot(m^2\cdot h\cdot bar)^{-1}$ is explained by the occurrence of additional defects (Fig. 11b).

After chemical treatment, one of the ceramic NF membranes had a visible crack in the glass seal layer on one edge of the membrane, see Fig. 12a. After repair with epoxy glue, the MWCO and the permeability of the membrane decreased to their original value (Fig. 11). This suggests that the additional defects, caused by sodium hypochlorite exposure, only occurred in the glass seal edges of this membrane. This hypothesis was tested by repeating the experiment for all membranes; similar effects were revealed for all membranes (Fig. 11).

It should be noted that after repair, no defects were measured in the membranes, while the pristine membranes contained 2–7% defects. Thus, the repair removed not only the additional defects due to the chemical treatment but also the initial defects. This suggests that the initial defects in the pristine membranes were also located in the glass seal layer, which explains the decrease of the corrected MWCO after repair compared to the pristine membranes. It should be noted that this conclusion does not apply for all pristine membranes; we cannot state that defects in pristine membranes e.g. the membranes analysed in Section 3.1 only occur on the glass seal layer.

These results thus suggest that the sodium hypochlorite damaged the silica glass seal layer on the edge of the membranes, which is also shown on the scanning electron microscope (SEM) image of the glass seal layer (Fig. 12b). Not only is the crack on the edge of the membrane visible in this picture but also the cracks in the entire silica glass seal

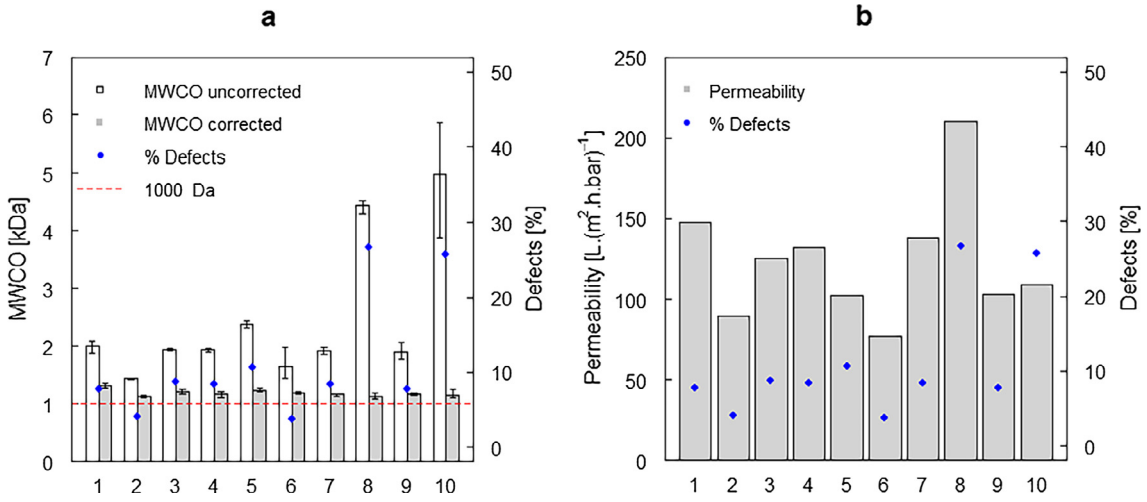

Fig. 7. (a–b): MWCO in kDa (a) and hydraulic permeability in $L\cdot(m^2\cdot h\cdot bar)^{-1}$ (b) of pristine ceramic tUF membranes. MWCO of disc membranes with a purchased cut-off of 1 kDa (red dashed line) was calculated without (white bars) and with correction for defects (grey bars). The percentages of defects in the membrane are shown (blue dots). The error bars represent the standard deviation of triplicate measurements. One batch is shown. (For interpretation of the references to colour in this figure legend, the reader is referred to the web version of this article.)

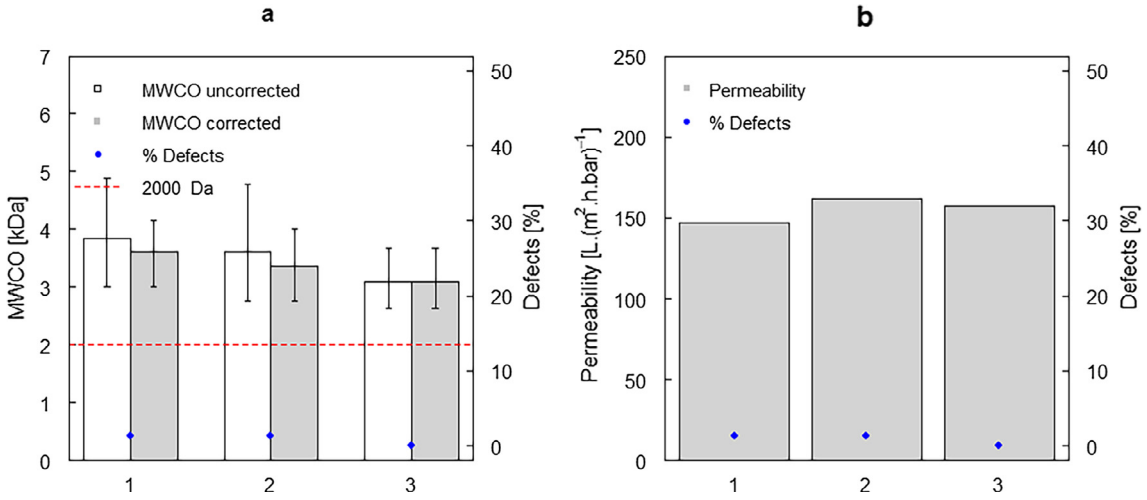

Fig. 8. (a–b): MWCO in kDa (a) and hydraulic permeability in $L \cdot (m^2 \cdot h \cdot bar)^{-1}$ (b) of pristine ceramic tUF membranes. MWCO of disc membranes with a purchased cut-off of 2 kDa (red dashed line) was calculated without (white bars) and with correction for defects (grey bars). The percentages of defects in the membrane are shown (blue dots). The error bars represent the standard deviation of triplicate measurements. One batch is shown. (For interpretation of the references to colour in this figure legend, the reader is referred to the web version of this article.)

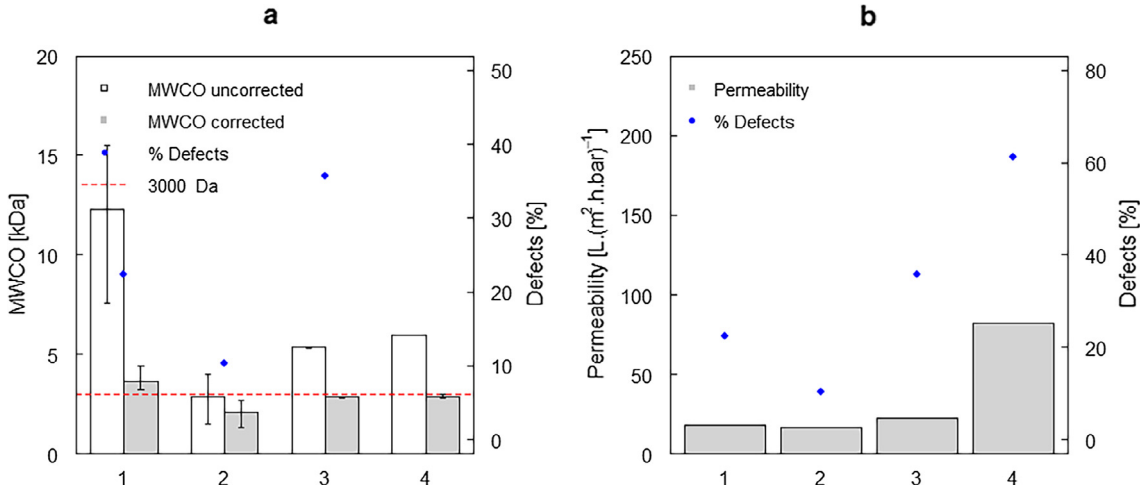

Fig. 9. (a-b): MWCO in kDa (a) and hydraulic permeability in $L \cdot (m^2 \cdot h \cdot bar)^{-1}$ (b) of pristine ceramic tUF membranes. MWCO of disc membranes with a purchased cut-off of 3 kDa (red dashed line) was calculated without (white bars) and with correction for defects (grey bars). The percentages of defects in the membrane are shown (blue dots). The error bars represent the standard deviation of triplicate measurements. One batch is shown. (For interpretation of the references to colour in this figure legend, the reader is referred to the web version of this article.)

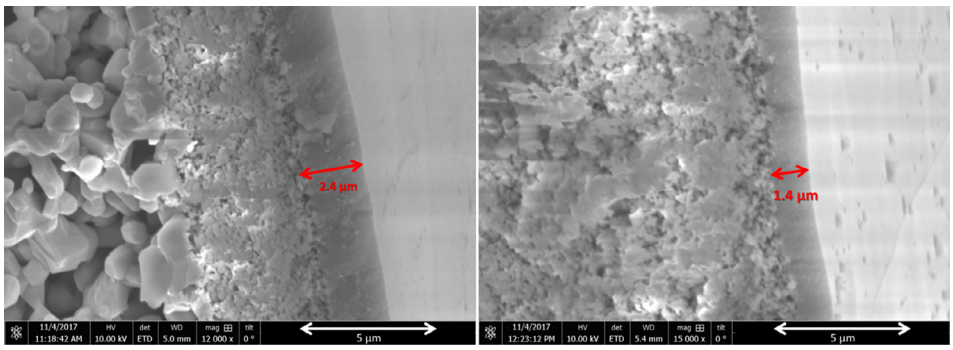

Fig. 10. (a–b): Scanning electron microscope (SEM) picture of the filtration surface of two different ceramic tUF membrane with a purchased cut-off of 3 kDa. The thickness of the layer varies from 1.4 to 2.4 µm.

layer.

Finally, the effect of more severe chemical cleaning with sodium hydroxide was investigated using 2% sodium hydroxide for 30 min at a temperature of 97 °C and a pH of 13.69. Fig. 13 shows that the hydraulic permeability and corrected MWCO increased after this chemical cleaning, and the epoxy glue at the edges of the membrane restored the values to the initial value. Thus, the higher concentration of sodium hydroxide also damaged the glass seal layer at the edges of the

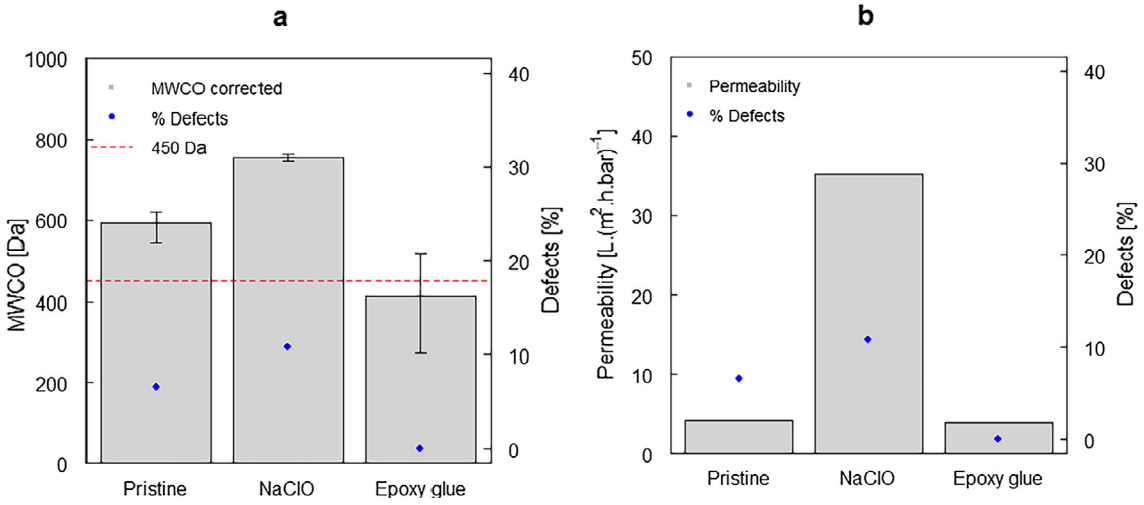

Fig. 11. (a–b): MWCO in kDa (a), permeability in $L{\cdot}(m^2{\cdot}h{\cdot}bar)^{-1}$ (b) and percentages of defects in tubular ceramic NF membranes with a purchased cut-off of 450 Da (red dashed line). The pristine membranes (Pristine) were treated with 1% sodium hypochlorite for 100 h (NaClO), then an epoxy glue layer was applied at the edges to cover the glass seal layer of the membranes (Epoxy glue). This experiment was executed four times, the data was averaged and the error bars represent the standard deviation of the different measurements. (For interpretation of the references to colour in this figure legend, the reader is referred to the web version of this article.)

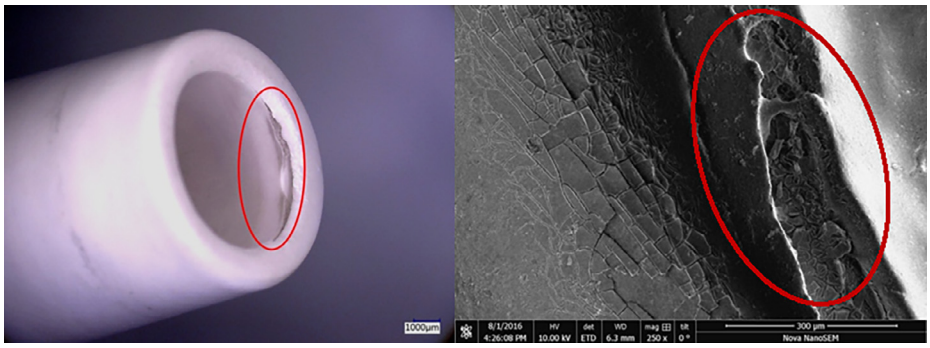

Fig. 12. (a–b): Ceramic NF membrane with a purchased cut-off of 450 Da after 100 h of chemical cleaning with 1% sodium hypochlorite shown with a digital microscope (a) and a scanning electron microscope (SEM) (b). A large crack is visible on the edge of the membrane (red circle) as well as small cracks throughout the silica glass seal layer.

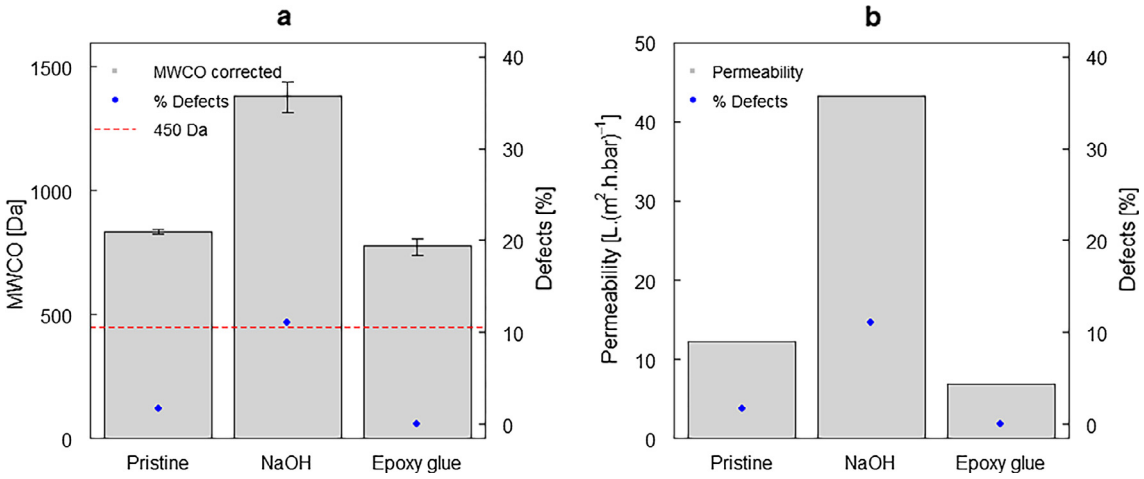

Fig. 13. (a–b): MWCO and permeability of tubular ceramic NF membranes with a purchased cut-off of 450 Da (red dashed line) when pristine (Before), treated with 2% sodium hydroxide (NaOH) for 30 min at 97 °C, and with end layer restored using epoxy glue (Glue). The error bars represent the standard deviation of triplicate measurements. (For interpretation of the references to colour in this figure legend, the reader is referred to the web version of this article.)

membranes, in a similar manner as the regular concentration of sodium hypochlorite, without affecting the separation layer. Van Gestel et al. performed similar long-term exposure experiments using NaOH for six weeks at a pH of 13 at 25 °C and did not detect damage on the membranes [4]. This indicates that a pH of 13 at 25 °C lies within the boundaries of chemical resistance of the ceramic NF membrane.

4. Conclusions

For the treatment of high organic load waste streams, it is important that the quality of ceramic tUF and NF are intact, for both pristine membranes and those after frequent chemical cleaning. An extension to the existing MWCO method was developed to quantify defects on

ceramic membranes. The quality and the robustness of a broad range of pristine ceramic tUF and NF membranes was investigated using this extension. The following conclusions can be drawn:

- Defects in membranes can be quantified using an extension to the commonly used MWCO method.
- Defects are frequently detected in the studied commercial ceramic membranes.
- The MWCO, both uncorrected and corrected, of pristine membranes varied often from the purchase cut-off, even within membranes from the same batch. This was tested with membranes of different pore sizes and geometries from various suppliers.
- The hydraulic permeability of pristine membranes varied notably for pristine membranes with a similar purchased cut-off.
- Long-term treatment with chemicals, especially sodium hypochlorite, damaged the tubular ceramic membranes, although this chemical is widely used to clean ceramic membranes. However, the chemicals only affected the glass seal layer on the edges of the membranes. Similar results were found using high concentrations of NaOH.
- Re-sealing of the edges of the membranes recovered the original properties of the tubular membranes. Moreover, the defects present in the pristine membranes were removed as well.

Acknowledgments

The research presented in this article was supported by the STW grant (Project Number 13346) and is part of the Rotterdam Innovative Nutrients Energy and Water (RINEW) project. The authors would like to thank *Evides Industriewater*. Moreover, thanks to Katie Friedman, Irene Caltran, Welldone Moyo, Antoine Brunet, Jingwen Li, Beatrice Scantamburlo, and Herman Kramer for their contribution to this research. Finally, we would like to acknowledge the anonymous reviewers whose comments were valuable to this manuscript.

References

[1] R. Weber, H. Chmiel, V. Mavrov, Characteristics and application of new ceramic nanofiltration membranes, Desalination 157 (2003) 113–125.
[2] M. Lee, Z. Wu, K. Li, 2 - Advances in ceramic membranes for water treatment, 2015. doi: http://dx.doi.org/10.1016/B978-1-78242-121-4.00002-2.
[3] K. Guerra, J. Pellegrino, Development of a techno-economic model to compare ceramic and polymeric membranes, Sep. Sci. Technol. 48 (2013) 51–65, https://doi.org/10.1080/01496395.2012.690808.
[4] T. Van Gestel, C. Vandecasteele, A. Buekenhoudt, C. Dotremont, J. Luyten, B. Van Der Bruggen, G. Maes, Corrosion properties of alumina and titania NF membranes, J. Memb. Sci. 214 (2003) 21–29, https://doi.org/10.1016/S0376-7388(02)00517-3.
[5] B. Van Der Bruggen, C. Vandecasteele, T. Van Gestel, W. Doyen, R. Leysen, A review of pressure-driven membrane processes in wastewater treatment and drinking water production, Environ. Prog. 22 (2003) 46–56, https://doi.org/10.1002/ep.670220116.
[6] M. Zebić Avdičević, K. Košutić, S. Dobrović, Effect of operating conditions on the performances of multichannel ceramic UF membranes for textile mercerization wastewater treatment, Environ. Technol. (United Kingdom) 38 (2017) 65–77, https://doi.org/10.1080/09593330.2016.1186225.
[7] I. Voigt, M. Stahn, S. Wöhner, A. Junghans, J. Rost, W. Voigt, Integrated cleaning of coloured waste water by ceramic NF membranes, Sep. Purif. Technol. 25 (2001) 509–512, https://doi.org/10.1016/S1383-5866(01)00081-8.
[8] M. Ebrahimi, N. Busse, S. Kerker, O. Schmitz, M. Hilpert, P. Czermak, Treatment of the bleaching effluent from sulfite pulp production by ceramic membrane filtration, Membranes (2015) 1–15, https://doi.org/10.3390/membranes6010007.
[9] N. Busse, F. Fuchs, M. Kraume, P. Czermak, Treatment of enzyme-initiated delignification reaction mixtures with ceramic ultrafiltration membranes: Experimental investigations and modeling approach, Sep. Sci. Technol. 51 (2016) 1546–1565, https://doi.org/10.1080/01496395.2016.1167739.
[10] A. Dafinov, J. Font, R. Garcia-Valls, Processing of black liquors by UF/NF ceramic membranes, Desalination 173 (2005) 83–90, https://doi.org/10.1016/j.desal.2004.07.044.
[11] G. Mustafa, K. Wyns, A. Buekenhoudt, V. Meynen, Antifouling grafting of ceramic membranes validated in a variety of challenging wastewaters, Water Res. 104 (2016) 242–253, https://doi.org/10.1016/j.watres.2016.07.057.
[12] Y. Thibault, J. Gamage McEvoy, S. Mortazavi, D. Smith, A. Doiron, Characterization of fouling processes in ceramic membranes used for the recovery and recycle of oil sands produced water, J. Memb. Sci. 540 (2017) 307–320, https://doi.org/10.1016/j.memsci.2017.06.065.
[13] M. Abbasi, A. Salahi, M. Mirfendereski, T. Mohammadi, A. Pak, Dimensional analysis of permeation flux for microfiltration of oily wastewaters using mullite ceramic membranes, Desalination 252 (2010) 113–119, https://doi.org/10.1016/j.desal.2009.10.015.
[14] M. Ebrahimi, S. Kerker, S. Daume, M. Geile, F. Ehlen, I. Unger, S. Schütz, P. Czermak, Innovative ceramic hollow fiber membranes for recycling/reuse of oilfield produced water, Desalin. Water Treat. 55 (2015) 3554–3567, https://doi.org/10.1080/19443994.2014.947780.
[15] F.L. Hua, Y.F. Tsang, Y.J. Wang, S.Y. Chan, H. Chua, S.N. Sin, Performance study of ceramic microfiltration membrane for oily wastewater treatment, Chem. Eng. J. 128 (2007) 169–175, https://doi.org/10.1016/j.cej.2006.10.017.
[16] K. Loganathan, P. Chelme-Ayala, M. Gamal El-Din, Effects of different pretreatments on the performance of ceramic ultrafiltration membrane during the treatment of oil sands tailings pond recycle water: A pilot-scale study, J. Environ. Manage. 151 (2015) 540–549, https://doi.org/10.1016/j.jenvman.2015.01.014.
[17] F.C. Kramer, R. Shang, S.G.J. Heijman, S.M. Scherrenberg, J.B. van Lier, L.C. Rietveld, Direct water reclamation from sewage using ceramic tight ultra- and nanofiltration, Sep. Purif. Technol. (2015) 1–21, https://doi.org/10.1111/j.1747-6593.2011.00271.x.Olsson.
[18] R. Shang, A.R.D. Verliefde, J. Hu, S.G.J. Heijman, L.C. Rietveld, The impact of EfOM, NOM and cations on phosphate rejection by tight ceramic ultrafiltration, Sep. Purif. Technol. 132 (2014) 289–294, https://doi.org/10.1016/j.seppur.2014.05.024.
[19] J. Garcia-Ivars, J. Dura-Maria, C. Moscardo-Carreno, C. Carbonell-Alcaina, M.I. Alcaina-Miranda, M.I. Iborra-Clar, Rejection of trace pharmaceutically active compounds present in municipal wastewaters using ceramic fine ultrafiltration membranes: Effect of feed solution pH and fouling phenomena, Sep. Purif. Technol. 175 (2017) 58–71, https://doi.org/10.1016/j.seppur.2016.11.027.
[20] J. Xu, C.Y. Chang, C. Gao, Performance of a ceramic ultrafiltration membrane system in pretreatment to seawater desalination, Sep. Purif. Technol. 75 (2010) 165–173, https://doi.org/10.1016/j.seppur.2010.07.020.
[21] Z. Cui, W. Peng, Y. Fan, W. Xing, N. Xu, Effect of cross-flow velocity on the critical flux of ceramic membrane filtration as a pre-treatment for seawater desalination, Chin. J. Chem. Eng. 21 (2013) 341–347, https://doi.org/10.1016/S1004-9541(13)60470-X.
[22] P.S. Goh, A.F. Ismail, A review on inorganic membranes for desalination and wastewater treatment, Desalination (2017), https://doi.org/10.1016/j.desal.2017.07.023.
[23] J. Xu, C.Y. Chang, J. Hou, C. Gao, Comparison of approaches to minimize fouling of a UF ceramic membrane in filtration of seawater, Chem. Eng. J. 223 (2013) 722–728, https://doi.org/10.1016/j.cej.2012.12.089.
[24] H. Guo, Y. Wyart, J. Perot, F. Nauleau, P. Moulin, Low-pressure membrane integrity tests for drinking water treatment: A review, Water Res. 44 (2010) 41–57, https://doi.org/10.1016/j.watres.2009.09.032.
[25] M. Huang, Y. Li, G. Gu, Chemical composition of organic matters in domestic wastewater, Desalination 262 (2010) 36–42, https://doi.org/10.1016/j.desal.2010.05.037.
[26] J. Shirley, S. Mandale, V. Kochkodan, Influence of solute concentration and dipole moment on the retention of uncharged molecules with nanofiltration, Desalination 344 (2014) 116–122, https://doi.org/10.1016/j.desal.2014.03.024.
[27] B. Van Der Bruggen, C. Vandecasteele, Modelling of the retention of uncharged molecules with nanofiltration, Water Res. 36 (2002) 1360–1368, https://doi.org/10.1016/S0043-1354(01)00318-9.
[28] S. Blumenschein, A. Böcking, U. Kätzel, S. Postel, M. Wessling, Rejection modeling of ceramic membranes in organic solvent nanofiltration, J. Memb. Sci. 510 (2016) 191–200, https://doi.org/10.1016/j.memsci.2016.02.042.
[29] S. Zeidler, P. Puhlfürß, U. Kätzel, I. Voigt, Preparation and characterization of new low MWCO ceramic nanofiltration membranes for organic solvents, J. Memb. Sci. 470 (2014) 421–430, https://doi.org/10.1016/j.memsci.2014.07.051.
[30] B. Hofs, J. Ogier, D. Vries, E.F. Beerendonk, E.R. Cornelissen, Comparison of ceramic and polymeric membrane permeability and fouling using surface water, Sep. Purif. Technol. 79 (2011) 365–374, https://doi.org/10.1016/j.seppur.2011.03.025.
[31] C. Causseranda, P. Aim, C. Vilani, T. Zambellib, Study of the effects of defects in ultrafiltration membranes on the water flux and the molecular weight cut-off, Desalination. 149 (2002) 485–491.
[32] H. Uchiyama, Evaporation-driven self-organization of sol-gel dip-coating films, J. Ceram. Soc. Jpn. (2015) 457–464, https://doi.org/10.2109/jcersj2.123.457.
[33] A. Buekenhoudt, Stability of porous ceramic membranes, Membr. Sci. Technol. 13 (2008) 1–31, https://doi.org/10.1016/S0927-5193(07)13001-1.
[34] M.C. Almecija, A. Martinez-Ferez, A. Guadix, M.P. Paez, E.M. Guadix, Influence of the cleaning temperature on the permeability of ceramic membranes, Desalination 245 (2009) 708–713, https://doi.org/10.1016/j.desal.2009.02.041.
[35] A. Buekenhoudt, F. Bisignano, G. De Luca, P. Vandezande, M. Wouters, K. Verhulst, Unravelling the solvent flux behaviour of ceramic nanofiltration and ultrafiltration membranes, J. Memb. Sci. 439 (2013) 36–47, https://doi.org/10.1016/j.memsci.2013.03.032.
[36] M. Mulder, Basic principles of membrane technology, Zeitschrift Für Phys. Chemie. (1996) 564, https://doi.org/10.1524/zpch.1998.203.Part_1_2.263.
[37] C.M. Tam, A.Y. Tremblay, Membrane pore characterization-comparison between single and multicomponent solute probe techniques, J. Memb. Sci. 57 (1991) 271–287, https://doi.org/10.1016/S0376-7388(00)80683-3.
[38] R. Shang, A. Goulas, C.Y. Tang, X. de Frias Serra, L.C. Rietveld, S.G.J. Heijman, Atmospheric pressure atomic layer deposition for tight ceramic nanofiltration membranes: Synthesis and application in water purification, J. Memb. Sci. 528 (2017) 163–170, https://doi.org/10.1016/j.memsci.2017.01.023.